Electronic structure and optical spectra of $LuInCu_4$ and $YbMCu_4$ (M=Cu, Ag, Au, Pd, and In)

V. N. Antonov,* M. Galli, and F. Marabelli
Istituto Nazionale per la Fisica della Materia (INFM) and Dip. di Fisica A. Volta, Universitá di Pavia, 27100 Pavia, Italy

A. N. Yaresko and A. Ya. Perlov
Institute of Metal Physics, 36 Vernadsky Street, 252142 Kiev, Ukraine

E. Bauer
Institut für Experimentalphysik, Technical University, A-1040 Vienna, Austria
(Received 3 December 1999)

Optical reflectivity measurements over a wide spectral range and at different temperatures together with self-consistent electronic band structure calculations have been used to investigate the electronic structure of the $LuInCu_4$ and $YbMCu_4$ (M=Cu,Ag,Au,Pd,In) compounds. The electronic structure of the compounds is investigated theoretically using an energy-band approach in combination with the linear-response formalism. The energy-band structure is obtained within the local-spin-density approximation (LSDA) and within its extension that explicitly takes into account the on-site $4f$ Coulomb interaction U (LSDA+U). A remarkable agreement between theory and experiment has been found.

I. INTRODUCTION

The $YbMCu_4$ (M=Cu, Ag, Au, Pd, and In) compounds crystallize in the cubic $AuBe_5$-type ($C15b$) structure and preserve the Yb ion in its trivalent state with total angular momentum $J=7/2$.[1,2] These systems have been investigated extensively because of their rich variety of phenomena at low temperature. In particular, $YbAgCu_4$ is known to show a typical dense Kondo behavior,[2,3] in which localized moments of Yb^{3+} ($4f^{13}$) at high temperatures are gradually screened through the hybridization with the conduction electrons, resulting in the enhanced Pauli paramagnetic state down to very low temperatures. A moderately large electronic specific heat coefficient has also been reported as $\gamma = 245$ mJ/mol K^2.[4] Recently prepared by a high-pressure technique the $YbCu_5$ phase with $C15b$ structure also shows Kondo-lattice formation[5] with an even larger electronic specific heat coefficient $\gamma=550$ mJ/mol K^2. Furthermore, the temperature dependence of magnetic susceptibility[2] and magnetic part of specific heat[3] in these systems are well described by the Bethe-ansatz solution of the Coqlin-Schrieffer model.[6] No magnetic ordering was found in both compounds down to 2.0 K.[5,7] On the other hand, the Kondo effect is not dominant in $YbAuCu_4$ and $YbPdCu_4$, and long range magnetic ordering is observed at 0.6 and 0.8 K, respectively.[2,8] Finally, $YbInCu_4$ has attracted much attention recently because it is the only known stoichiometric compound that undergoes a first-order isostructural valence transition at ambient pressure.[1,9–11] At high temperature Yb appears to be essentially trivalent, displaying Curie-Weiss susceptibility with a paramagnetic moment near free ion value of $4.5\mu_B$. At the first-order valence transition (occurring at a temperature T_v in the range from about 40 to 80 K, depending sensitively on the particular composition of each sample.[12] For our sample $T_v=42$ K) the Yb valence is reduced to approximately 2.8 (as estimated by x-ray-absorption and lattice constant measurements[9,13]), with a consequent increase in lattice volume of 0.5% and a reduction in magnetic susceptibility and spin-disorder scattering.[10] High-resolution neutron powder-diffraction studies confirm that the first-order transition is an isostructural one, with $YbInCu_4$ retaining its $C15b$ structure at all temperatures.[14,15] Such an ''isomorphic'' valence transition is fundamentally similar to the $\alpha\rightarrow\gamma$ transition in cerium,[16] which raises the question whether both transitions have a common origin.

Optical spectroscopy has been proved as a powerful tool in the study of intermediate-valence and heavy-fermion compounds[17–20] because it supplies direct information about the energy states (both occupied and unoccupied) in a wide energy interval around the Fermi energy and can provide a means of discrimination between the different theoretical limits. The optical properties of the $YbMCu_4$ (M=Ag, Au, Pd, and In) were investigated in Refs. 21–23. In the case of $YbInCu_4$ relevant differences in the optical spectrum were observed between 0.1 and 2 eV, above and below the transition temperature.[21]

The energy-band structure for $YbInCu_4$ together with $LuInCu_4$ has been presented first in Ref. 24 using the self-consistent augmented plane wave (APW) method with the local-spin-density approximation (LSDA). In $LuInCu_4$, the calculations show that this compound is a compensated semimetal with small carrier density. LSDA produces for $YbInCu_4$ the energy-band structure with fully occupied $4f$ bands located in the vicinity of the Fermi level. In other words, the LSDA gives a divalent state for the Yb ion in contradiction to the experimental data, according to which at high temperature Yb appears to be essentially trivalent and after the phase transition at $T_v=42$ K the Yb valence is reduced to approximately 2.8.[9,13] The calculations of the electronic structure of $YbMCu_4$(M=Ag,Au, Pd) in Refs. 23 and 25 in the LSDA using the full-potential linearized APW (FP LAPW) method also produce the band structure with $4f$ states situated below the Fermi level at $\sim$0.5 eV. Direct measurements of the electronic structure of $YbMCu_4$ (M=Ag, Au, Pd) compounds using x-ray photoemission (XPS)

and bremsstrahlung isochromat spectroscopies (BIS) suggested that the valence of Yb in this compounds is close to 3+ with occupied $4f$ states situated between -12 to -5 eV and an unoccupied hole state just above and close to the Fermi level.[26] The application of LSDA calculations to the YbXCu$_4$ is inappropriate, because of the correlated nature of $4f$ electrons in these compounds. The LSDA gave the wrong energy position for $4f$ energy bands and predicted a divalent ground state for the Yb ion in these compounds in contrast to the experimental data.

The aim of this paper is to present a detailed experimental and theoretical study of the electronic structure and optical properties of YbMCu$_4$ (M=Cu, Ag, Au, Pd, and In) compounds. The energy-band structure of the compounds calculated within the *ab initio* approach takes strong correlations into account. This is achieved by applying a local-spin-density approximation to the density-functional theory supplemented by a Hubbard U term (LSDA+U).[27] We also presented the electronic structure and optical spectra of LuInCu$_4$ as a reference compound.

The paper is organized as follows. The computational details are presented in Sec. II. Section III presents the optical measurements of the compounds. Section IV is devoted to the electronic structure of the compounds calculated in the LSDA and LSDA+U approximations. Theoretical results are compared to previous band-structure calculations and the experimental measurements. Finally, the results are summarized in Sec. V.

II. THEORETICAL FRAMEWORK

The application of standard LSDA methods to f-shell systems meets with problems in most cases, because of the correlated nature of the f electrons. To account better for the on-site f-electron correlations, we have adopted as a suitable model Hamiltonian that of the LSDA+U approach.[27] The main idea is the same as in the Anderson impurity model:[28] the separate treatment of localized f electrons for which the Coulomb f-f interaction is taken into account by a Hubbard-type term in the Hamiltonian $\frac{1}{2}U\Sigma_{i\neq j}n_in_j$ (n_i are f-orbital occupancies), and delocalized s,p,d electrons for which the local density approximation for the Coulomb interaction is regarded as sufficient. The detailed description of the LSDA+U method can be found elsewhere;[27,29,30] here we only mention that the orbital energies ε_i are determined in the LSDA+U method as derivatives of total energy functional E with respect to orbital occupations n_i:

$$\varepsilon_i=\frac{\partial E}{\partial n_i}=E_{LSDA}+(U-J)(\tfrac{1}{2}-n_i)=E_{LSDA}+U_{eff}(\tfrac{1}{2}-n_i), \tag{1}$$

where U is the screened Coulomb parameter, and J is the exchange parameter. This simple formula shifts the LSDA orbital energy by $-U_{eff}/2$ for occupied f orbitals ($n_i=1$) and by $+U_{eff}/2$ for unoccupied f orbitals ($n_i=0$).

The advantage of the LSDA+U method is the ability to treat simultaneously delocalized conduction band electrons and localized $4f$ electrons in the same computational scheme. With regard to these electronic structure calculations, we mention that the present approach is still essentially a single particle description, even though intra-atomic $4f$-Coulomb correlations are explicitly taken into account. The LSDA+U method has proven to be a very efficient and reliable tool in calculating the electronic structure of systems containing localized orbitals where the Coulomb interaction is much larger than the bandwidth. It works not only for $4f$ orbitals of rare-earth ions, but also for such systems as transition metal oxides, where localized $3d$ orbitals hybridize quite strongly with oxygen $2p$ orbitals (see review article Ref. 29), it was also successfully applied to heavy-fermion compounds YbPtBi (Ref. 31) and Yb$_4$As$_3$ (Ref. 32).

RMCu$_4$ (R=Yb, Lu; M=Cu, Ag, Au, Pd, In) compounds are isostructural to MgSnCu$_4$, which has a face-centerd cubic (fcc) lattice with six atoms per unit cell. The space group is $F\bar{4}3m$ (No. 216) with R at the $4c$ positions, M at the $4a$ positions, and Cu at the $16e$ positions. The experimental lattice constants are equal to 6.975, 7.0814, 7.0519, 7.0396, and 7.123 Å for Cu, Ag, Au, Pd, and In, respectively.[33]

The electronic structure of the compounds was calculated self-consistently using the local-spin-density approximation[34] and the fully relativistic spin-polarized LMTO method[35–37] in the atomic-sphere approximation, including the combined correction (ASA+CC).[35,38] Core-charge densities were recalculated at every iteration of the self-consistency loop. The spin polarization has been included in the variational step.[39] The combined correction terms have been included also in calculation of the optical matrix elements.[40] The basis consisted of the Yb s, p, d, f, and g; Cu s, p, d, and f; Ms, p, and d LMTO's. The energy expansion parameters $E_{\nu Rl}$ were chosen at the centers of gravity of the occupied parts of the partial densities of states both for charge density calculations and for MO calculations. The k-space integrations were performed with the improved tetrahedron method[41] and charge self-consistently was obtained with 589 irreducible **k** points.

We have adopted the LSDA+U method[27] as a different level of approximation to treat the electron-electron correlation. Note that U_{eff} is simply a parameter and set to 6.0 eV for all the compounds (according to experiment, as described below).

In our optical calculations we calculated the dielectric function considering only electronic excitations. We used the random-phase approximation and neglected local-field and finite lifetime effects.[42] The interband contribution to the imaginary part of the dielectric function is given by

$$\varepsilon_2^{\nu\nu}(\omega)=\frac{8\pi^2e^2}{m^2\omega^2}\sum_{n\neq n'}^{unocc}\sum_{n'}^{occ}\int_{BZ}|P^{\nu}_{nn'}(\mathbf{k})|^2\delta \times(E_n^{\mathbf{k}}-E_{n'}^{\mathbf{k}}-\hbar\omega)\frac{d^3k}{(2\pi)^3} \tag{2}$$

where $P^{\nu}_{nn'}(\mathbf{k})$ is the projection of the momentum matrix elements $P_{nn'}(\mathbf{k})$ along the ν direction of the electric field **E**. $E_n^{\mathbf{k}}$ are the one-electron energies. The relativistic expression of the optical transition matrix element in Dirac representation was derived in Ref. 40.

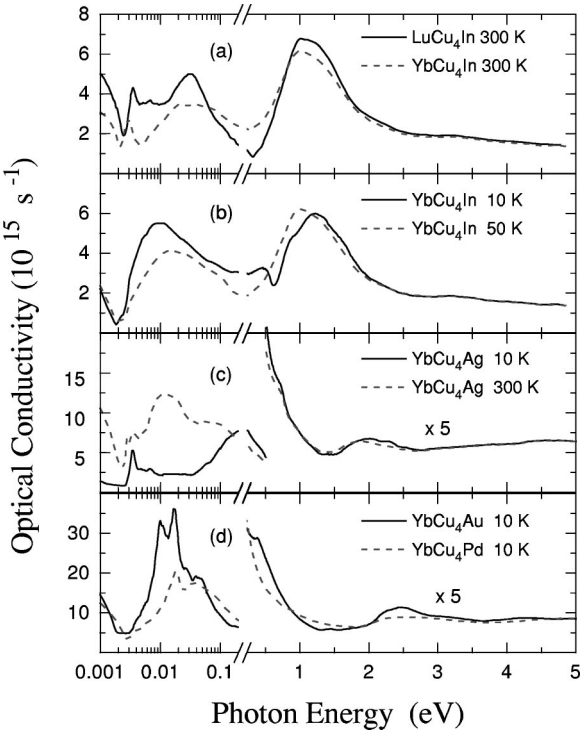

FIG. 1. Optical conductivity of the four Yb compounds and $LuCu_4In$ measured at different temperatures.

After having evaluated Eq. (2), we calculate the interband contribution to the real part of the dielectric function $\varepsilon_1(\omega)$ from the Kramers-Kronig (KK) relation:

$$\varepsilon_1(\omega)=1+\frac{2}{\pi}\mathrm{P}\int\frac{\varepsilon_2(\omega')\omega' d\omega'}{\omega'^2-\omega^2}, \tag{3}$$

where P stands for the principal value. Finally, we add the intraband contribution to obtain the total complex dielectric function. We neglect this contribution to $\varepsilon_2(\omega)$ according to the perfect crystal approximation (the defects and lattice oscillations are absent). The intraband contribution to $\varepsilon_1(\omega)$ is given by

$$\varepsilon_1^{\nu\nu}(\omega)_{intra}=1-\frac{(\omega_p^{\nu\nu})^2}{\omega^2}, \tag{4}$$

where the squared plasma frequency is given by

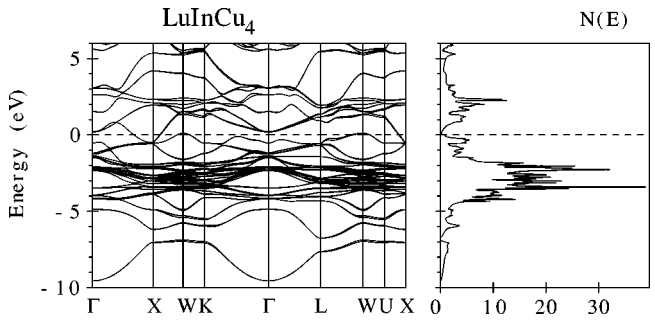

FIG. 2. LSDA self-consistent fully relativistic, spin-polarized energy band structure and total DOS [in states/(unit cell eV)] of $LuInCu_4$.

$$(\omega_p^{\nu\nu})^2=\left(\frac{e}{\pi\hbar}\right)^2\sum_n\int_{BZ}d^3k[\partial E_n^{\mathbf{k}}/\partial k^\nu]^2\delta(E_n^{\mathbf{k}}-E_f). \tag{5}$$

We also calculated the optical conductivity and the reflectivity $R(\omega)$ using Eqs. (2)–(5) and the following relations:

$$\sigma(\omega)=\frac{\omega}{4\pi}\varepsilon_2(\omega), \tag{6}$$

and

$$R(\omega)=\left|\frac{\sqrt{\tilde{\varepsilon}}-1}{\sqrt{\tilde{\varepsilon}}+1}\right|^2 \tag{7}$$

where the complex dielectric function $\tilde{\varepsilon}=\varepsilon_1+\varepsilon_2$.

We first calculate directly the imaginary part of dielectric function (2) in a wide energy range from 0 to 40 eV. The real part of the dielectric function and the other optical functions were then calculated using the formulas presented above.

III. EXPERIMENTAL MEASUREMENTS

The samples were prepared from stoichiometric amounts of elements using high-frequency melting under a protective argon atmosphere. Subsequently, a heat treatment at $T=750\,^\circ$C 1 week long, in argon atmosphere, was applied. The phase purity of the samples was checked using x-ray diffraction measurements which were also used to determine the lattice parameters. A shining optically cleaned surface of about 0.5 cm^2 was obtained on each sample by mechanical polishing with diamond powders.

Due to the tendency to oxidation of the surfaces, freshly polished surfaces were prepared just before the sample measurements and checks of the oxide effects on the optical measurements were performed by repeating the experiment. No surface effects seem to affect the results below 3 eV; for larger energies a decrease of the absolute reflectance can occur due to roughness.

Usual grating photospectrometers and spectroscopic ellipsometry were used to measure the optical reflectivity of our samples from the near infrared up to the ultraviolet (6 eV). Below 0.6 eV a Fourier spectrometer allowed us to extend the measured spectral range down to far infrared (~2 meV). Measurements were performed at room temperature and at 6 K in the far infrared; at room temperature and at 10 K in the other spectral ranges. In the case of $YbInCu_4$ a further measurement was performed at about 50 K, just above the valence transition of this sample.

Spectroscopic ellipsometry at ambient temperature were also applied over the range 1.4–5 eV. Since ellipsometry is, in general, very sensitive to oxide layers and not sensitive to small roughness, the comparison of reflectance and ellipsometric results allows a monitoring of the surface conditions.

Kramers-Krönig analysis of the data has been performed in order to obtain the real and imaginary parts of the dielectric function $\tilde{\epsilon}=\epsilon_1+i\epsilon_2$. Below 2 meV an extrapolation based on the Drude model was assumed in order to connect our results with the measured values of the dc conductivity σ_{dc}.[43–45] Beyond 6 eV we use a conventional extrapolation with a term decreasing as ω^s, where the exponent s has been

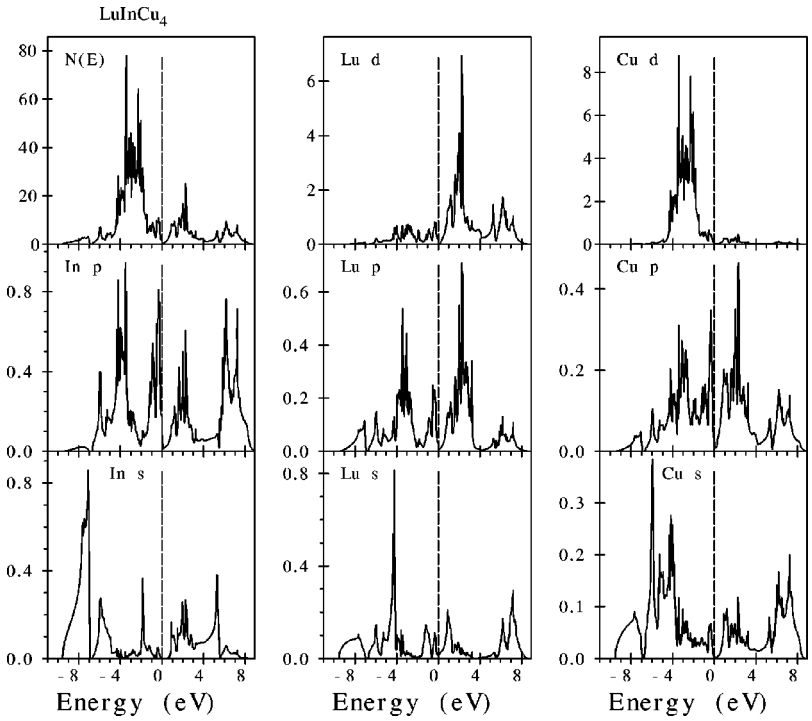

FIG. 3. LSDA total $N(E)$ [in states/(unit cell eV)] and partial DOS [in states/(atom eV)] of $LuInCu_4$.

adjusted to fit the values of the dielectric function independently obtained by spectroscopic ellipsometry over the range 1.4–5 eV.

The optical conductivity $\sigma(\omega)=(\omega/4\pi)\epsilon_2(\omega)$ for the investigated compounds is plotted in Fig. 1. The low- and high-energy parts of the spectra are indicated by a break of the energy scale.

At low energies, between 1 and 500 meV, all panels in Fig. 1 display a minimum at the extreme left of the energy scale followed by a peak, or a shoulder, at about 3–4 meV. Similar features were revealed also in the spectra of the reference compound $YInCu_4$.[46] They have to be ascribed to an optical phonon (the peak) and to the semimetallic character of this series of compounds. In fact, due to the low carrier density and to the character of the electronic states at the Fermi level, originated essentially from *d* states of Yb/Lu and *s*,*p* states of the metallic ions, the electron-phonon interaction causes a strong frequency-dependent scattering which produces the conductivity minimum observed in the spectra. Such a feature has, therefore, nothing to do with a direct renormalization of the states related to the *f*-*d* hybridization of the incomplete *f* shell of ytterbium, as instead observed in other heavy-fermion or Kondo systems.[17]

The spectral behavior at energies above 10 meV exhibits a common trend although different details, in the energy and in the intensity of the optical structures, can be distinguished among the various materials in the low- and high-temperature regimes. Thus the broad peak or shoulder extending roughly up to 0.1 eV is followed, at increasing energies, by a decrease of the optical conductivity in all compounds. This decrease corresponds to the high-energy limit for the free carrier contribution to the optical conductivity.

A striking exception to this behavior is the 10 K spectrum of $YbAgCu_4$ [Fig. 1(c)] between 10 and 200 meV. Actually, $YbAgCu_4$ at the lowest temperatures exhibits Kondo-lattice behavior and a strong renormalization of the electronic states near the Fermi energy is expected. As a matter of fact, according to Refs. 22 and 23, a renormalized plasma frequency $\omega_p^*=\sqrt{\epsilon_o}\omega_p=4e^2k_F^3/3\pi m^*\approx 0.35$ eV, corresponding to an effective mass $m^*\approx 44m_e$ and a Kondo temperature T_K

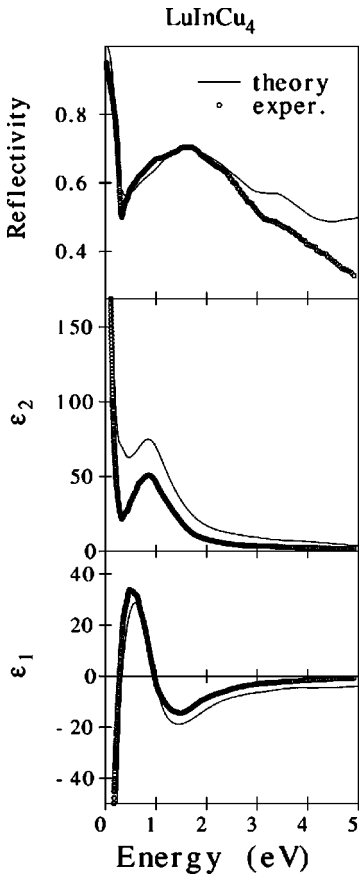

FIG. 4. Comparison between the experimental (dots) and calculated optical reflectivity $R(\omega)$, real part $\varepsilon_1(\omega)$ and imaginary part $\varepsilon_2(\omega)$ of the dielectric function of $LuInCu_4$ calculated within LSDA (solid line).

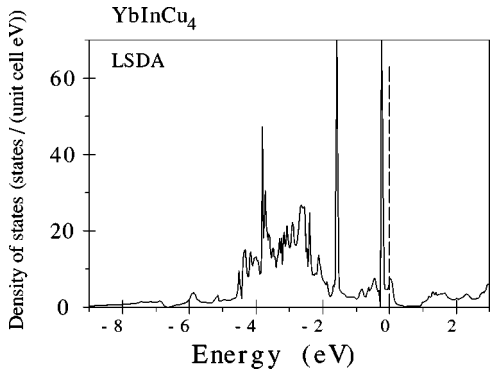

FIG. 5. LSDA total DOS of $YbInCu_4$ in states/(unit cell eV).

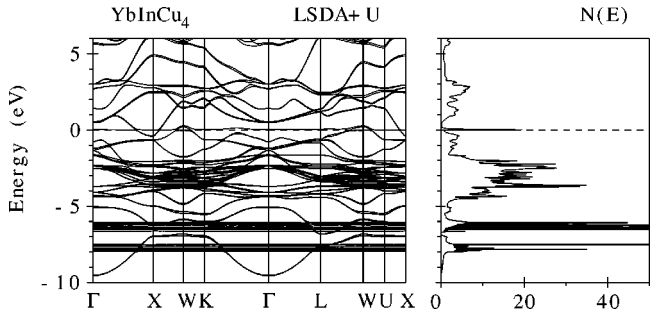

FIG. 6. LSDA+U self-consistent fully relativistic, spin-polarized energy band structure and total DOS [in states/(unit cell eV)] of $YbInCu_4$ ($U_{eff}=6$ eV).

≈90 K, can be evaluated from the optical spectrum.[22] Such a value of T_K is not far from that estimated by other techniques.[45,47]

Moving to the high-energy part of the spectra in Fig. 1, one can observe a series of structures corresponding to interband transitions. A shoulder at about 0.4 eV is observed for Au and Ag compounds at room temperature, which is absent in the spectrum of the Pd compound. A further structure appears in the Ag spectrum at 0.9 eV.

A series of smooth optical structures centred at 2 and 4.3 eV occur in $YbAgCu_4$. Analogous structures are found in $YbAuCu_4$ and $YbPdCu_4$ at 2.5, 3, 4.2, and 5.2 eV with higher intensity in the former compound, and at 2.5 eV and as a smooth single structure, with lower intensity, between 4 and 6 eV in the latter compound.

The spectra of Lu- and Yb-based ternary compounds of In deserve separate comments. In fact, Lu- and Yb-based materials at room temperature exhibit almost exactly the same features except a broader and smoother intraband contribution in $YbInCu_4$ (due to the additional magnetic scattering similar to $YbAgCu_4$). In both $YbInCu_4$ and $LuInCu_4$ at high T, a conductivity minimum at 0.3 eV is followed, at increasing energy, by an intense, probably double but not resolved structure centered at 1 eV [see Fig. 1(a)]. A shoulder at ~2 eV and a second smooth peak at about 3.1 eV can also be observed.

By decreasing the temperature below 40 K, an abrupt change occurs in the optical response of $YbInCu_4$ between 0.1 and 2 eV [see Fig. 1(b)]. The minimum present at 0.3 eV in Fig. 1(a) disappears and the optical conductivity assumes larger values up to about 0.5 eV, where a structure occurs. A net decrease of the peak intensity at 1 eV on the low-energy side is compensated by an increase above 1.1 eV, so that the 1 eV peak in Fig. 1(a) moves to ≃1.3 eV in the 10 K spectrum in Fig. 1(b). Such a behavior is consistent with the change observed in the Yb valence,[9] which can change the carrier density and therefore the Fermi level.

IV. ELECTRONIC STRUCTURE AND INTERBAND TRANSITIONS

The LSDA fully relativistic spin-polarized energy band structure and total and partial density of states (DOS) of $LuInCu_4$, are shown in Figs. 2 and 3. These results agree

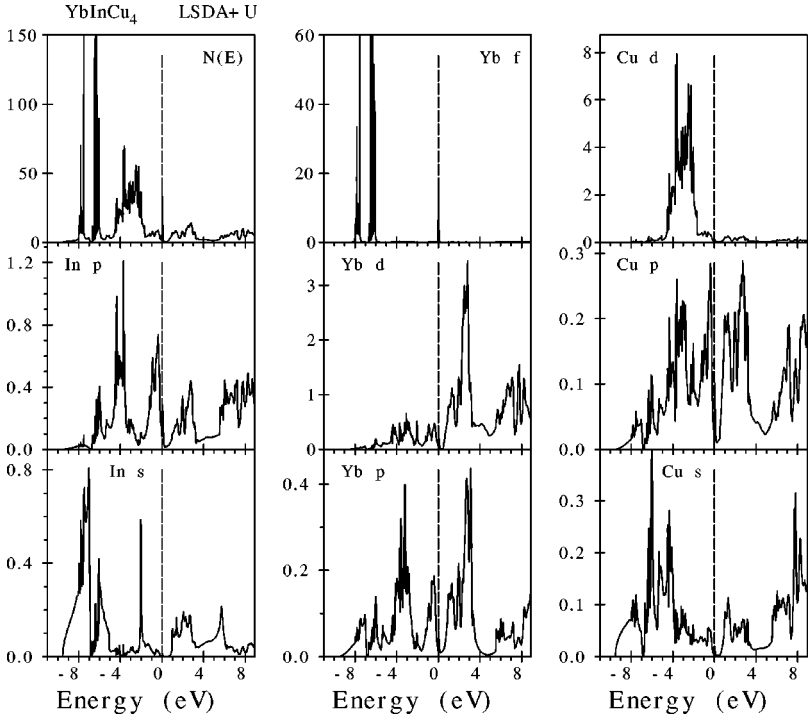

FIG. 7. LSDA+U total $N(E)$ [in states/(unit cell eV)] and partial DOS [in states/(atom eV)] of $YbInCu_4$.

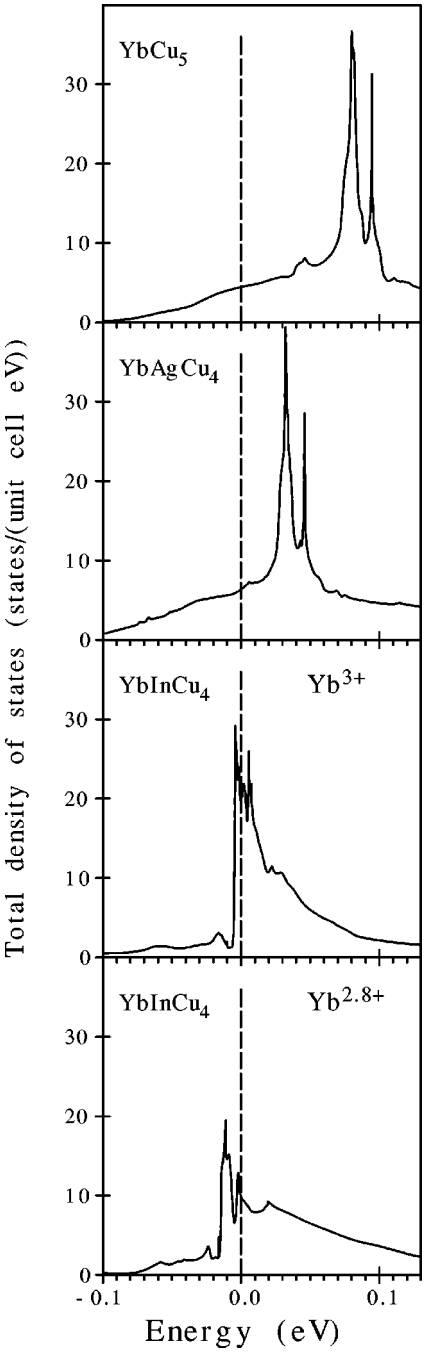

FIG. 8. Expended view of the total DOS $N(E)$ of $YbCu_5$, $YbAgCu_4$, and $YbInCu_4$ (for Yb^{3+} and $Yb^{2.8+}$ configurations) calculated in the LSDA+U approximation.

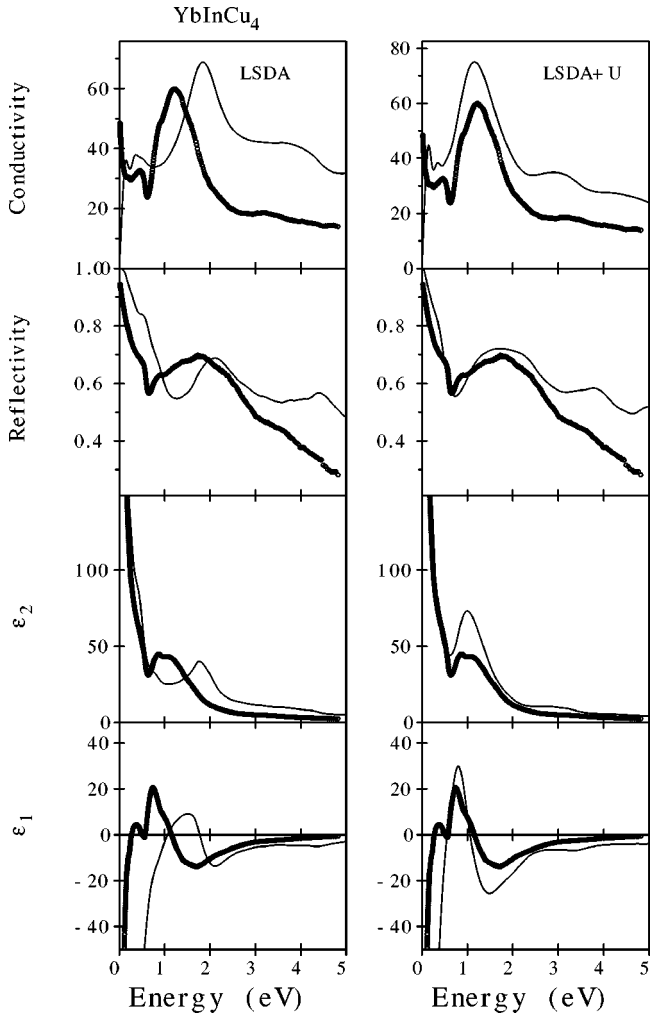

FIG. 9. Comparison between the experimental (dots) optical conductivity $\sigma(\omega)$ (in 10^{14} s^{-1}), reflectivity R, real part $\varepsilon_1(\omega)$, and imaginary part $\varepsilon_2(\omega)$ of the dielectric function of $YbInCu_4$ calculated within LSDA and LSDA+U approximations (solid line).

well with previous band-structure calculations by Takegahara and Kasuya.[24] The calculated energy band structure shows that $LuInCu_4$ is a compensated semimetal with small carrier density in agreement with electrical resistivity and Hall effect measurements.[45] The Fermi surface consists of two sheets. The 32nd band has closed hole sheets h_{32} around W symmetry points and the 33rd band has closed electron sheets e_{33} around X points. The bands in the lowest region of the occupied part of the band structure of $LuInCu_4$ (Fig. 3) between -9.5 and -7 eV have mostly In s character with some amount of Cu and Lu sp character mixed in. The highest region can be characterized as a bonding combination of Cu d and In p states. Cu d bands are completely occupied and situated below the Fermi level at -4 to -1.5 eV. Lu d states are almost empty and situated above the Fermi level.

In Fig. 4 we compare the calculated complex dielectric function $\varepsilon(\omega)$ and the reflectivity $R(\omega)$ with the experiment. As can be seen, theory in LSDA and experiment agree very well. Above 3 eV, the theory gives a slightly larger reflectivity in comparison with experimental measurements. One of the possible reasons for this is a nonideal sample surface; its roughness could reduce the optical reflectivity in this energy range.

The LSDA total DOS of $YbInCu_4$ is shown in Fig. 5. The energy-band structure of $YbInCu_4$ is very similar to that of $LuInCu_4$. The bands in the lowest region have mostly In s character with some amount of Cu and Yb s character mixed in. Cu d bands are completely occupied and situated below the Fermi level between -4 and -1.5 eV. The large narrow peak close to the Fermi energy is formed by Yb $4f$ states. Unoccupied $5d$ bands of Yb are separated from the $4f$ states by a quasigap, a characteristic and important feature of the $YbInCu_4$ compound. The position of the LSDA $4f$ states close to the Fermi energy is, on the other hand, in contradiction to the findings of XPS and BIS experiments.[26]

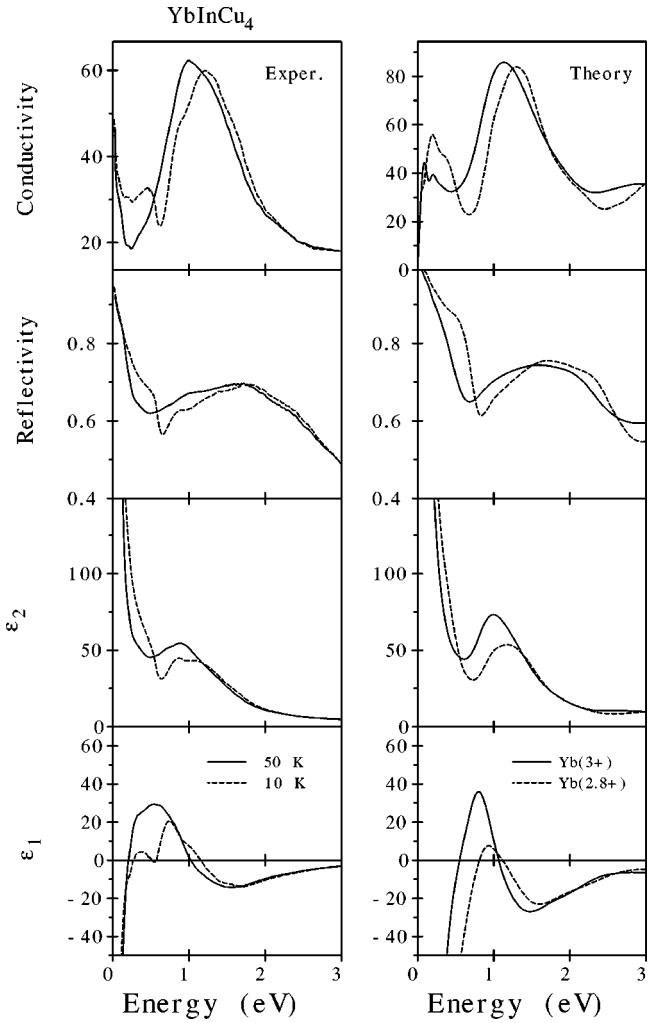

FIG. 10. Comparison between the experimental optical spectra of $YbInCu_4$ measured below (10 K) and above (50 K) the phase transition and calculated spectra for different occupation numbers of the hole $4f$ state in the LSDA+U approximation.

In our spin-polarized fully relativistic LMTO LSDA+U band-structure calculations we start from the $4f^{13}$ configuration for Yb^{3+} ion with 13 on-site $4f$ energies shifted downwards by $U_{\rm eff}/2$ and one level shifted upwards by this amount. From total energy calculations we found that the Yb^{3+} ground state corresponds to the projection of the orbital momentum onto the spin direction equal to $m_l=+3$ in accordance with all three Hund's rules. The energies of occupied and unoccupied Yb^{3+} f bands are separated by approximately $U_{\rm eff}$. We emphasize, however, that the $4f$ states are not treated as completely localized. They may hybridize, and together with all other states their energy positions relax to self-consistency.

Usually the Hubbard-like $U_{\rm eff}$ is estimated by comparing the theoretically calculated energy positions of f bands with XPS and UPS measurements. From photoemission measurements $U_{\rm eff}$ is found to be in the range of 5–7 eV for different Yb compounds.[48] It can also be calculated from atomic Dirac-Hartree-Fock (DHF) calculations,[48] from Green-function impurity calculations,[49] and from band-structure calculations in supercell approximation.[50] The calculated value of $U_{\rm eff}$ strongly depends on theoretical approximations

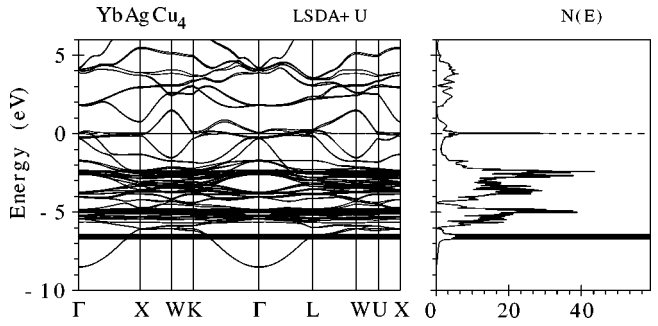

FIG. 11. LSDA+U self-consistent fully relativistic, spin-polarized energy-band structure and total DOS [in states/(unit cell eV)] of $YbAgCu_4$ ($U_{eff}=6$ eV).

and we prefer to treat the value of $U_{\rm eff}$ as a parameter and try to specify it from comparison of the calculated physical properties of YbMCu$_4$ compounds with experiments.

The LSDA+U energy bands and partial density of states of $YbInCu_4$ for $U_{\rm eff}=6$ eV are shown in Figs. 6 and 7. For the trivalent Yb ion, thirteen $4f$ electron bands are well below the Fermi level in the energy range between -6 and -8 eV (Fig. 7). They are split due to spin-orbit coupling $\Delta\epsilon_{so}=1.2$ eV and separated from a $4f$ hole state by the correlation energy $U_{\rm eff}$. The unoccupied $4f^{14}$ level, which, through the Coulomb interaction is initially placed above E_F, is pulled on E_F during the process of self-consistent relaxation. A fundamental aspect of this observation is that we find the pinning of the $4f^{14}$ state at E_F to be an inherent property of $YbInCu_4$: It happens irrespective of the precise value of U_{eff}. The insensitiveness of this feature on U_{eff} can be understood as reflecting the large bandwidth of the In p band with a low DOS and the existence of a quasigap just above the Fermi level. The $4f$ hole level should become partially occupied to achieve the required number of electrons within the Fermi sphere. Due to a small phase space for hybridization and small Yb $4f$–In p orbital overlap, the DOS peak of the hole band is as narrow as 0.02 eV (Fig. 8).[51] It is now clear why the usual Kondo-lattice scenario is inappropriate for this compound. For a Kondo resonance to develop both the occupied and empty $4f$ states must be sufficiently far away from the Fermi level. Quite opposite to this situation the (almost) empty level is pinned to the Fermi energy. Since the upper $4f$ level is only partly occupied, $YbInCu_4$ is calculated to be an intermediate valent compound in agreement with the experimental data.[1,9–11]

After the consideration of the above band-structure properties we turn to the optical spectra. In Fig. 9 we show the LSDA and LSDA+U calculated and experimental optical spectra of $YbInCu_4$. The best agreement between theory and the experiment was found when we used the LSDA+U approximation. The most important discrepancy in the LSDA spectra is the shifting of the prominent peak in the optical conductivity and imaginary part of dielectric function $\varepsilon_2(\omega)$ towards larger photon energies. This peak situated at ~ 1.2 eV in the experimentally measured optical spectra is mostly due to In $p\rightarrow$Yb d interband transitions. These transitions take place between occupied and empty energy bands along L-W, X-W, and Γ-K symmetry directions and also in some inner parts of the Brillouin zone. Although $4f$ states do not participate to the optical interband transitions in the en-

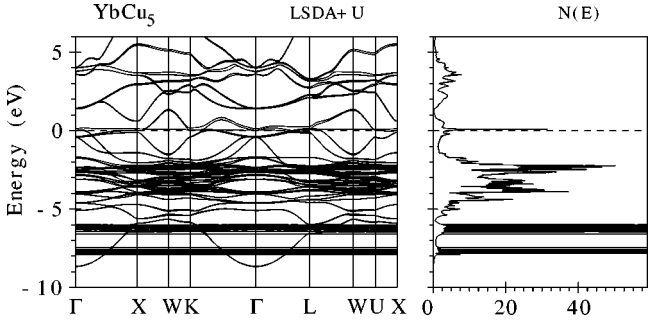

FIG. 12. LSDA+U self-consistent fully relativistic, spin-polarized energy band structure and total DOS [in states/(unit cell eV)] of $YbCu_5$ ($U_{eff}=6$ eV).

ergy interval from 0 to 5 eV (due to a large binding energy of occupied $4f$ states and the extreme narrowness of the partly occupied hole $4f^{14}$ level), they affect the optical spectra indirectly through changing of the ionicity of the Yb ion. LSDA produces the energy-band structure of $YbInCu_4$ with fully occupied $4f$ bands for divalent Yb ions (Fig. 5). The Coulomb repulsion U_{eff} strongly influences the electronic structure of $YbInCu_4$. Thirteen $4f$ occupied energy bands are well below the Fermi energy and a hole $4f^{14}$ level is partly occupied and pinned at the Fermi level. Therefore the ionicity of the Yb ion in the LSDA+U calculations is close to 3+. On the other hand, the $4f$-electron density is closer to the nucleus than that of the $4s$, p, and d electrons. Hence, the increasing Yb ionicity (i.e., the decreasing number of $4f$ electrons in the close vicinity of the nucleus) in the LSDA $+U$ calculations leads to narrowing of Yb d energy bands due to decreasing of nucleus screening. Therefore empty Yb d states in the LSDA+U calculations shift downwards decreasing the In $p\rightarrow$Yb d interband energies and the prominent peak shifts to smaller energies in remarkable agreement with the experimental measurements (Fig. 9).

The measurements of the optical spectra of $YbInCu_4$ in Ref. 21 show that its optical response abruptly changes at the phase transition temperature (Fig. 10), whereas no distortion of the crystal structure occurs. The major effect of such a phenomenon is also due to the changing of the Yb ionicity. As estimated by x-ray-absorption and lattice constant measurements[9,13] at the first-order valence transition at $T_v=42$ K the Yb valence is reduced to approximately 2.8. In order to investigate the influence of the valence reduction of Yb, we performed the self-consistent LSDA+U calculations of the energy-band structure and optical spectra of $YbInCu_4$ using starting configurations of the unoccupied $4f^{14}$ level equal to 0.9 and 0.8. Such a ''virtual crystal approximation''[52] leads to the energy-band structure with wider Yb d energy bands due to the increasing nuclear screening by $4f$ electrons. The optical spectra, therefore, are shifted towards higher photon energies in good agreement with the experimental measurements (Fig. 10).

The LSDA+U calculations show that the decrease of the Yb ionicity is accompanied by an essential decrease of the density of states at the Fermi level, which is equal to 17.0, 11.5, and 10.8 states/(unit cell eV) for Yb^{3+}, $Yb^{2.9+}$, and $Yb^{2.8+}$, respectively (Fig. 8). This aspect reflects the fact that the ground state of $YbInCu_4$ exhibits a Yb valence less than 3+. Here, we should mention that for the Yb^{3+} configuration we mean the starting configuration with zero occupation of $4f^{14}$ level. In the process of self-consistent relaxation the initially empty hole $4f^{14}$ level becomes partly occupied due to pinning at the Fermi level with an occupation number equal to 0.14 (valence $v=2.86$). Using the $Yb^{2.9+}$ configuration as initial configuration we achieved—after the self-consistent calculations—an occupation number equal to 0.24. These results are in a good agreement with x-ray absorption measurements at the Yb L_{III} edge, which gave $v(L_{III})=2.9$ and 2.8 above and below T_v, respectively.[9]

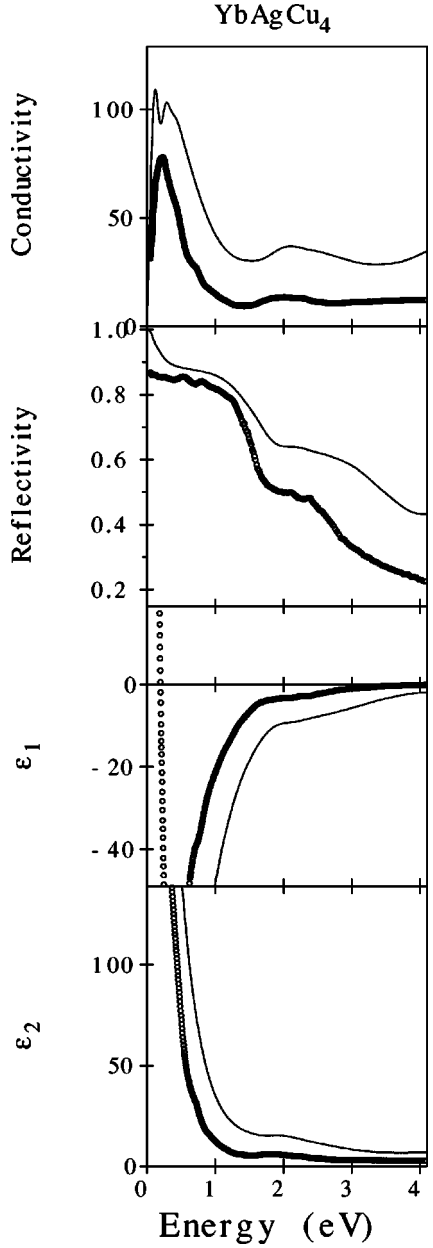

FIG. 13. Comparison between the experimental (dots) and LSDA+U calculated (solid line) optical spectra of $YbAgCu_4$.

The total DOS at the Fermi level, resulting essentially from the $4f$ hole states, yields for $U_{\rm eff}=6$ eV a bare band contribution to the Sommerfeld constant of $\gamma=\pi^2k_B^2N_AN(\epsilon_F)/3=40$, 27, and 25.4 mJ mol^{-1} K^{-2} for Yb^{3+}, $Yb^{2.9+}$, and $Yb^{2.8+}$, respectively, in good agreement with specific heat measurements.[9] These measurements gave $\gamma=22.3$ mJ mol^{-1} K^{-2} at low temperatures below the phase

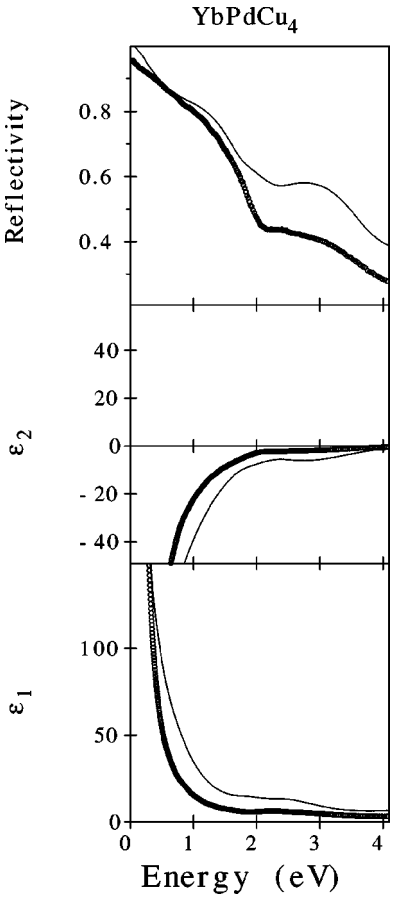

FIG. 14. Comparison between the experimental (dots) and LSDA+U calculated (solid line) optical spectra of $YbPdCu_4$.

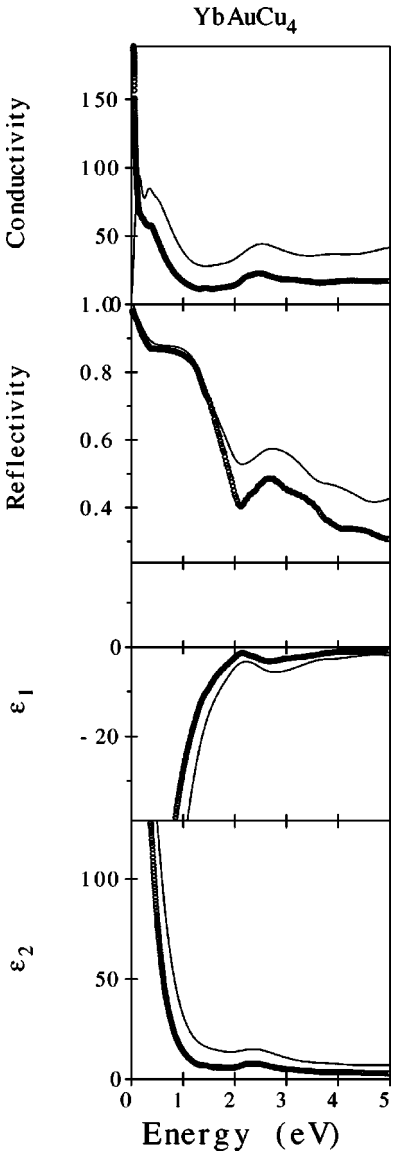

FIG. 15. Comparison between the experimental (dots) and LSDA+U calculated (solid line) optical spectra of $YbAuCu_4$.

transition. The specific heat is also abruptly increased at the phase transition temperature $T_v = 42$ K.[9]

As an example, we show the LSDA+U energy bands of $YbAgCu_4$ and $YbCu_5$ for $U_{\text{eff}} = 6$ eV in Figs. 11 and 12. The energy-band structure of $YbAgCu_4$ as well as of $YbCu_5$ is similar to $YbInCu_4$ (Fig. 6). For the trivalent Yb ion, thirteen $4f$ electron bands are well below the Fermi level in the energy range between -4.5 and -7 eV slightly shifted upwards in comparison with $YbInCu_4$. They are split due to spin-orbit coupling $\Delta\epsilon_{so} = 1.5$ eV and separated from the $4f$ hole state by the correlation energy U_{eff}. The position of occupied $4f$ bands in $YbAgCu_4$ is in good agreement with x-ray photoemission measurements. According to the XPS measurements the multiplet structure of the $4f^{12}$ final states on Yb^{3+} sites is situated between -5 and -12 eV.[26] The most significant difference between the electronic structures of $YbAgCu_4$ and $YbInCu_4$ compounds is in the position of the hole $4f^{14}$ level. In the case of $YbInCu_4$ the upper $4f$ level is partly occupied and pinned at the Fermi level due to the existence of a quasigap in the density of states just above the Fermi level (Fig. 6). In $YbAgCu_4$ the occupied $4f$ states shifted upward, and a similar quasigap situated 1.5 eV above the Fermi energy (Fig. 11); therefore the hole level in $YbAgCu_4$ is completely empty and situated sufficiently far from the Fermi level (Fig. 8). Such a situation is appropriate for the developing of the Kondo-lattice scenario in this compound. The hole level has a similar position in $YbCu_5$ (Fig. 8), $YbPdCu_4$, and $YbAuCu_4$. $YbCu_5$ is really a typical dense Kondo system with an electronic specific heat coefficient $\gamma = 550$ mJ/mol K^2 (Ref. 5), while the Kondo effect is not the most dominant interaction mechanism in $YbAuCu_4$ and $YbPdCu_4$, where long range magnetic ordering is observed at 0.6 and 0.8 K, respectively.[2]

In Figs. 13, 14, and 15 we show the LSDA+U calculated and experimentally measured optical spectra of $YbAgCu_4$, $YbPdCu_4$, and $YbAuCu_4$. The agreement between the theory and the experiment is very good.

V. SUMMARY

In conclusion we have shown that the optical spectra of $YbMCu_4$ (M=Cu, Ag, Au, Pd, and In) are very sensitive tools for drawing conclusions about the appropriate model description. On account of the calculated optical spectra we conclude that $YbInCu_4$ optical spectra are best described using the LSDA+U approach. It was found that the main peak in the optical conductivity $\sigma(\omega)$ of $YbMCu_4$ at 1.2 eV results from In $p \rightarrow$ Yb d interband transitions between occu-

pied and empty energy bands along L-W, X-W, and Γ-K symmetry directions and also in some inner parts of the Brillouin zone.

Measurements of the optical spectra of $YbInCu_4$ show significant changes at the phase transition temperature, in particular between 0.1 and 0.2 eV. The theoretical calculations demonstrate that the major effect results from the change of the Yb ionicity. At the first-order valence transition at $T_v = 42$ K the Yb valence is reduced from 2.9 to approximately 2.8. This leads to an increase of the nuclear screening by $4f$ electrons and to an increase of the In $p \rightarrow$Yb d interband transition energies due to the shift of the empty Yb d band upwards.

In $YbInCu_4$ the upper hole $4f$ level is partly occupied and pinned at the Fermi energy, therefore, $YbInCu_4$ is calculated to be an intermediate valent compound in agreement with the experimental data. In the YbMCu$_4$ (M=Cu, Ag, Au, and Pd) a hole level is completely empty and situated sufficiently far from the Fermi level. Such a situation is appropriate for the developing of the Kondo-lattice scenario.

The different ground states observed in YbMCu$_4$ (M=Cu, Ag, Au, and Pd) compounds result from the competition between three interactions: the crystal field interaction, the magnetic intersite Ruderman-Kittel-Kasuya-Yosida interaction, and the intrasite Kondo effect. The evaluation of ground states of the compounds from first principles requires further investigation.

ACKNOWLEDGMENTS

V.N.A. gratefully acknowledges the hospitality during his stay at Universitá di Pavia.

*Permanent address: Institute of Metal Physics, 36 Vernadskii strasse, 252142 Kiev, Ukraine.

[1] K. Kojima, H. Hayashi, A. Minami, Y. Kasamatsu, and T. Hihara, J. Magn. Magn. Mater. **81**, 267 (1989).
[2] C. Rossel, K.N. Yang, M.B. Maple, Z. Fisk, E. Zingiebl, and J.D. Thomson, Phys. Rev. B **35**, 1914 (1987).
[3] M.J. Besnus, P. Haen, N. Hamdaoui, A. Herr, and A. Mayer, Physica B **163**, 571 (1990).
[4] N. Tsujii, J. He, K. Yoshimura, K. Kosuge, H. Michor, K. Kreiner, and G. Hischer, Phys. Rev. B **55**, 1032 (1997).
[5] N. Tsujii, J. He, F. Amita, K. Yoshimura, K. Kosuge, H. Michor, G. Hischer, and T. Goto, Phys. Rev. B **56**, 8103 (1997).
[6] V.T. Rajan, Phys. Rev. B **51**, 308 (1983).
[7] A. Severing, A.P. Murani, J.D. Thomson, Z. Fisk, and C.K. Loong, Phys. Rev. B **41**, 1739 (1990).
[8] E. Bauer, P. Fischer, F. Marabelli, M. Ellerby, K.A. McEwen, B. Roessli, and M.T. Fernandes-Dias, Physica B **234-236**, 676 (1997).
[9] I. Felner, I. Nowik, D. Vaknin, U. Potzel, J. Moser, J. Kalvius, G.M. Worthmann, G. Schmeister, G. Hitscher, E. Gratz, C. Schmitzer, N. Pilmayer, K.G. Prasad, H. de Waard, and H. Pino, Phys. Rev. B **35**, 6956 (1987); I. Felner and I. Nowik, *ibid.* **33**, 617 (1986); I. Nowik *et al.*, *ibid.* **37**, 5623 (1988).
[10] J.L. Sarrao, C.D. Immer, Z. Fisk, J.M. Lawrence, D. Madrus, and J.D. Thompson, Phys. Rev. B **54**, 12 207 (1996).
[11] B. Kindler, D. Finsterbusch, R. Graft, F. Ritter, W. Assmus, and B. Luthi, Phys. Rev. B **50**, 704 (1994).
[12] A. Löffert, M.L. Aigner, and W. Assmus, Cryst. Res. Technol. **34**, 267 (1999).
[13] A.L. Cornelius, J.M. Lawrence, J.L. Sarrao, Z. Fisk, M.F. Hundley, G.H. Kwei, J.D. Thompson, C.H. Booth, and F. Bridges, Phys. Rev. B **56**, 7993 (1997).
[14] J.M. Lowrence, G.H. Kwei, J.L. Sarrao, Z. Fisk, D. Madrus, and J.D. Thompson, Phys. Rev. B **54**, 6011 (1996).
[15] K. Kojima, Y. Nakai, T. Suzuki, H. Asano, F. Izumi, T. Fujita, and T. Hihara, J. Phys. Soc. Jpn. **59**, 792 (1990).
[16] J.W. Allen and L.Z. Liu, Phys. Rev. B **46**, 5047 (1992).
[17] F. Marabelli and P. Wachter, Phys. Scr. **45**, 120 (1992).
[18] S. Bocelli, F. Marabelli, and E. Bauer, Physica B **199-200**, 34 (1994).
[19] F. Marabelli, G.B. Parravicini, and F. Salghetti, Phys. Rev. B **52**, 1433 (1995).
[20] E. Bauer, R. Hauser, A. Galatanu, H. Michor, G. Hilscher, J. Sereni, M.G. Berisso, P. Pedrazzini, M. Galli, F. Marabelli, and P. Bonville, Phys. Rev. B **60**, 1238 (1999).
[21] M. Galli, F. Marabelli, and E. Bauer, Physica B **230-232**, 304 (1997); F. Marabelli and E. Bauer, J. Appl. Phys. **73**, 5418 (1993).
[22] M. Galli, F. Marabelli, and E. Bauer, Physica B **206-207**, 355 (1995).
[23] A. Continenza, P. Monachesi, M. Galli, F. Marabelli, and E. Bauer, Phys. Scr. **66**, 177 (1996); A. Continenza, P. Monachesi, M. Galli, F. Marabelli, and E. Bauer, J. Appl. Phys. **79**, 6423 (1996).
[24] K. Takegahara and T. Kasuya, J. Phys. Soc. Jpn. **59**, 3299 (1990).
[25] P. Monachesi and A. Continenza, Phys. Rev. B **54**, 13 558 (1996).
[26] J.S. Kang, J.W. Allen, C. Rassel, C.I. Seaman, and M.B. Maple, Phys. Rev. B **41**, 4078 (1990).
[27] V.I. Anisimov, J. Zaanen, and O.K. Andersen, Phys. Rev. B **44**, 943 (1991).
[28] P.W. Anderson, Phys. Rev. **124**, 41 (1961).
[29] V.I. Anisimov, F. Aryasetiawan, and A.I. Lichtenstein, J. Phys.: Condens. Matter **9**, 767 (1997).
[30] V.N. Antonov, B.N. Harmon, A.Ya. Perlov, and A.N. Yaresko, Phys. Rev. B **59**, 14 561 (1999).
[31] P.M. Oppeneer, V.N. Antonov, A.N. Yaresko, A.Ya. Perlov, and H. Eschrig, Phys. Rev. Lett. **78**, 4079 (1997).
[32] V.N. Antonov, A.N. Yaresko, A.Ya. Perlov, P. Thalmeier, P. Fulde, P.M. Oppeneer, and H. Eschrig, Phys. Rev. B **58**, 9752 (1998).
[33] P. Villars and L.D. Calvert, *Pearson's Handbook of Crystallographic Data for Intermetallic Phases* (ASM International, Materials Park, OH, 1991).
[34] U. von Barth and L.A. Hedin, J. Phys. C **5**, 1692 (1972).
[35] O.K. Andersen, Phys. Rev. B **12**, 3060 (1975); D.D. Koelling and B.N. Harmon, J. Phys. C **10**, 3107 (1977).
[36] V.V. Nemoshkalenko, A.E. Krasovskii, V.N. Antonov, Vl.N. Antonov, U. Fleck, H. Wonn, and P. Ziesche, Phys. Status Solidi B **120**, 283 (1983).
[37] V.N. Antonov, A.Ya. Perlov, A.P. Shpak, and A.N. Yaresko, J. Magn. Magn. Mater. **146**, 205 (1995).
[38] V.V. Nemoshkalenko and V.N. Antonov, *Computational Methods in Solid State Physics* (Gordon and Breach, London, 1998).
[39] H. Ebert, Phys. Rev. B **38**, 9390 (1988).
[40] V.N. Antonov, A.I. Bagljuk, A.Ya. Perlov, V.V. Nemoshkalenko,

Vl.N. Antonov, O.K. Andersen, and O. Jepsen, J. Low Temp. Phys. **19**, 494 (1993).
[41] P.E. Blöchl, O. Jepsen, and O.K. Andersen, Phys. Rev. B **49**, 16 223 (1994).
[42] H. Ehrenreich and M.H. Cohen, Phys. Rev. **115**, 786 (1959).
[43] E. Bauer, R. Hauser, E. Gratz, K. Payer, G. Oomi, and T. Kagayama, Phys. Rev. B **48**, 15 873 (1993).
[44] E. Bauer, E. Gratz, R. Hauser, Le Tuan, A. Galatanu, A. Kottar, H. Michor, W. Perthold, G. Hilscher, T. Kagayama, G. Oomi, N. Ichimiya, and S. Endo, Phys. Rev. B **50**, 9300 (1994).
[45] E. Bauer, Adv. Phys. **40**, 417 (1991).
[46] M. Galli, F. Marabelli, and E. Bauer, Phys. Rev. B **53**, 9517 (1996).
[47] G. Polatsek and P. Bonville, Z. Phys. B: Condens. Matter **88**, 189 (1992).
[48] J.F. Herbst and J.W. Wilkins, in *Handbook of the Physics and Chemistry of Rare Earths*, edited by K.A. Gschneidner, L. Eyring, and S. Hüfner (North-Holland, Amsterdam, 1987), Vol. 10, p. 321.
[49] P.H. Dederichs, S. Blügel, R. Zeller, and H. Akai, Phys. Rev. Lett. **53**, 2512 (1984).
[50] V.I. Anisimov and O. Gunnarsson, Phys. Rev. B **43**, 7570 (1991).
[51] We mention that quite recently it was shown, on the basis of LSDA+U electronic structure calculations, that in Yb-Bi-Pt a somewhat similar $4f$ hole level pinning occurs (Ref. 31). In Yb-Bi-Pt, however, the $4f$ hole level has even less hybridization with Bi p bands, which leads to a huge band-structure contribution to the Sommerfeld constant γ.
[52] J.M. Ziman, *Models of Disorder: The Theoretical Physics of Homogeneously Disordered Systems* (Cambridge University Press, Cambridge, 1979).